Journal of Magnetism and Magnetic Materials 565 (2023) 170215

Contents lists available at ScienceDirect

Journal of Magnetism and Magnetic Materials

journal homepage: www.elsevier.com/locate/jmmm

Glassy correlated state induced by disorder in the frustrated antiferromagnet $Tb_2Zr_2O_7$

J.G.A. Ramon [a], P.L.O. Silva [a], J.S. Gardner [b], R.S. Freitas [a,*]

[a] Instituto de Física, Universidade de São Paulo, 05314-970 São Paulo, SP, Brazil
[b] Material Science & Technology Division, Oak Ridge National Laboratory, Oak Ridge, TN 37831, USA

ARTICLE INFO

Keywords:
Magnetic frustration
Spin glass
Zirconate
Fluorite

ABSTRACT

We study the low-temperature thermomagnetic properties of the polycrystalline material $Tb_2Zr_2O_7$ through ac susceptibility and specific heat measurements. This zirconate displays a defect-fluorite structure in which the magnetic Tb^{3+} and nonmagnetic Zr^{4+} cations sit randomly on the same metal sublattice. No long-range magnetic order is found down to 100 mK, although dominant antiferromagnetic interactions are observed and the spins remain dynamic down to the lowest temperatures investigated. We observed a frequency-dependent peak around 2.5 K which is well described by many models of a canonical spin-glass transition. In-field specific heat measurements and the recovered entropy of the system $R\ln(4)$ suggest a two doublets ground state separated by 7 K. Comparisons to the pyrochlores $Tb_2Ti_2O_7$ and $Tb_2Hf_2O_7$ reinforce the collective spin-glass-type behavior and the opening for discussions of an exotic Coulomb phase in this material.

1. Introduction

Spin systems and the underlying geometry of their lattice structures, pertinent to their competing magnetic interactions, have drawn enormous interest and extensive investigations during the current millennium. The phenomenon known as geometrically frustrated magnetism is a crucial topic in condensed matter physics for displaying a broad spectrum of highly correlated magnetic phases [1–3]. Competition between nearest neighbors and further interactions, together with the arrangement of the magnetic sites all play an important role in selecting the ground states in the frustrated magnets. Such a scenario precludes the system from establishing a long-range order at very low temperatures, with a spin configuration of the ground state possessing an extremely large degeneracy. The ultimate example of a frustrated magnet is the quantum spin liquid, in which the spins remain fluctuating and the expected order is not reached even down to T = 0 K [4,5]. The concept of frustration is central to other studies including negative thermal expansion of materials, soft matter, and protein folding kinetics [6].

Experimental realizations of frustrated magnets are the $R_2M_2O_7$ pyrochlore oxides, in which R^{3+} is a magnetic rare-earth ion (e.g., Ho, Dy, Er, Tb) and M^{4+} is a transition metal or a *p*-block metal ion (e.g., Ti, Zr, Sn, Ge), both residing on two separated lattices of corner-sharing tetrahedra. These materials are perfectly suited for experimental investigations since they exist in form of large high-purity single crystals, and their large magnetic moments are appealing to neutron scattering studies. The rare-earth titanates with a diverse set of exotic phenomena include the spin ice compounds $Dy_2Ti_2O_7$ and $Ho_2Ti_2O_7$, with strong Ising-like anisotropy and dipolar interactions [7,8], in which Coulombic interactions between emergent magnetic monopole excitations exist [9,10]; the XY antiferromagnet $Er_2Ti_2O_7$, where an unconventional long-range order is induced by quantum fluctuations [11,12]; the Heisenberg antiferromagnet $Gd_2Ti_2O_7$ possessing partial ordering of their spins and fluctuations [13,14], and the unusual dynamics in $Yb_2Ti_2O_7$, previously a possible quantum spin liquid state candidate [15], that exhibits a multiphase magnetism [16].

One frustrated magnet that stands out among pyrochlore oxides is $Tb_2Ti_2O_7$. The vast interest in this material lies in that the Tb^{3+} spins remain dynamic in concert without developing long-range order in energy scales as low as 50 mK. This occurs despite its antiferromagnetic Curie-Weiss temperature Θ_{CW} = -19 K [17,18] and strong power-law magnetic correlations present at low temperatures, as reported by neutron studies [19,20]. It is proposed that this material has a spin-liquid ground state [18,21]. The magnetic Tb^{3+} in $Tb_2Ti_2O_7$ possesses a strong Ising-like crystalline electric field (CEF) anisotropy [17,22,23] analogous to the reported ones for spin ices $Dy_2Ti_2O_7$ [7,24] and

* Corresponding author.
E-mail address: freitas@if.usp.br (R.S. Freitas).

https://doi.org/10.1016/j.jmmm.2022.170215
Received 23 August 2022; Received in revised form 4 November 2022; Accepted 19 November 2022
Available online 23 November 2022

$Ho_2Ti_2O_7$ [25,26]. However, in $Tb_2Ti_2O_7$, the energy of its low-lying CEF levels is an order of magnitude smaller than those in the spin ices. The spatial arrangement of spins, along with the Ising single ion properties of Tb^{3+} and the antiferromagnetic correlations, conspire to generate a fluctuating ground state [27]. Measurements of the ac and dc magnetic susceptibility in zero applied field revealed a slowing down of the spin dynamics at 300 mK [21,28,29]. In the presence of a magnetic field, Ueland *et al.* [30] reported frequency-dependent peaks around 25 K on the real and imaginary parts of the ac susceptibility indicating unexpected slow spin relaxations and a collective magnetism. The dynamical ground state appears to be robust to disorder with reports of a spin-liquid state with quantum and quadrupolar effects in $Tb_{2+x}Ti_{2-x}O_{7+y}$ [31,32]. The search for spin liquid materials has accelerated over the past two decades and many materials have attractive characteristics. Disorder can be used as a tuning parameter and it can help elucidate some fractionalization features of the ground state. For example, a broad peak in the magnetic diffraction pattern from neutron experiments is a first indicator of novel spin liquids [2,18].

In fact, with frustration and different magnetic interactions in play, disorder appears as a novel probe employed by researchers to understand collective magnetic states. Disorder in the lattice such as defects, vacancies, random sites, and impurities is crucial to moving forward the physics concerning exotic magnetism and liquid systems [33]. Defects of oxygen-disorder nature have been reported to be of key importance for originating excitations in pyrochlore materials [34,35]. For example, in the oxygen-deficient $Dy_2Ti_2O_{7-\delta}$, the anisotropy of the Dy^{3+} changes from easy axis to easy plane in the presence of oxygen vacancy [34], and when a monopole hops next to a dysprosium tetrahedron with an oxygen vacancy, it results in a decrease of the system's energy and the trapping of monopoles [34]. In $Tb_2Hf_2O_7$, the anion disorder breaks the local symmetry around the Tb^{3+} cation sited in the pyrochlore lattice [35]. From neutron studies, no long-range magnetic order is found down to 100 mK [35,36], and the scattering pattern is reported to be the response of a Coulomb spin liquid supporting antiferromagnetic and power-law correlations over many terbium tetrahedra [35,36]. Moreover, inside this highly correlated phase, there is a spin glass transition at ~ 750 mK that emerges from its inherent structural defects [35].

A road to disorder in the long-range pyrochlore structure of the titanates $R_2Ti_2O_7$ is accomplished by introducing a larger *M* cation, such the ratio of ionic radii r_R/r_M is smaller than 1.46 [2,37]. Similarly, the stuffing of the *R* cations into the Ti^{4+} lattice was reported to lead to cation mixing of the independent tetrahedral networks [38,39]. As a result, a structural phase transition occurs from pyrochlore to defect fluorite between the members of the titanate rare-earth series, and the cell parameter is reduced to half its value [37,40]. The defect-fluorite structure is identified with a disorder of the cations *R* and *M*, occupying a single indistinct 4a site [37,41], see inset Fig. 1, and the environment around them consists of oxygen anions at 8c positions [37,41]. In this configuration, there is one oxygen vacancy, and for both cations, the average oxygen coordination number is 7 [37,42].

The canonical spin glass ground state is found when magnetic frustration and disorder coexist [43]. In this type of magnetic material, the magnetic moments became frozen and are arranged in a disordered configuration [43]. In the pyrochlores, despite an unclear source of randomness, there are some species with spin glass features. Well-known examples are $Y_2Mo_2O_7$ [44–48] and $Tb_2Mo_2O_7$ [44,49–51], both exhibiting a spin glass transition below 25 K. If disorder is expected in the family of XY pyrochlore antiferromagnets, it induces regions of clusters of spin glass as shown by Monte Carlo simulations [52]. For comparison, large-scale simulations find a finite-temperature spin-glass phase transition for Ising spins in 3D, and a much smaller temperature phase transition for XY and Heisenberg 3D spin glasses [53,54].

Investigations on the zirconate rare-earth series $R_2Zr_2O_7$ are attracting high interest recently, due to the exotic magnetism being reported in many of these compounds. For instance, in $Nd_2Zr_2O_7$, an antiferromagnetic all-in all-out ordering together with a fluctuating

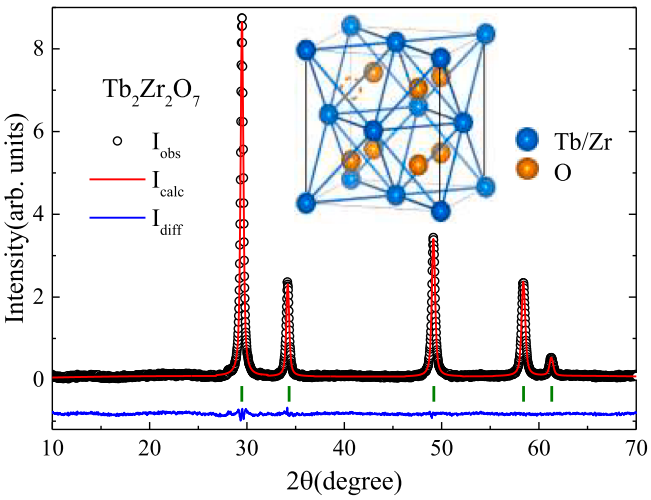

Fig. 1. X-ray diffraction pattern and calculated profile for $Tb_2Zr_2O_7$. Small vertical lines indicate peak positions of the disordered fluorite structure. Inset: The disordered fluorite structure with their *R*/*M* (Tb/Zr) cations at the 4a site (light blue spheres), and the oxygen anions at the 8c site when occupied (orange spheres) and vacant (dashed circle).

Coulomb phase was reported below 285 mK [55,56]. In $Pr_2Zr_2O_7$, spin-ice-like correlations and disorder-induced a possible quantum spin liquid state [57,58]. Many zirconium based 227 materials crystalize into the cubic pyrochlore structure, stabilized for *R* cations with an ionic radius larger than the Gd ion [37]. On the other hand, its closely related defect fluorite structure is formed by a smaller *R*, for which the cations are completely mixed creating significant disorder [2,37]. Some defect-fluorite examples include $Er_2Zr_2O_7$, which exhibits a spin glass-like transition at ~ 600 mK [59], $Dy_2Zr_2O_7$, possessing nearest neighbor correlations and fast spin dynamics to the lowest temperatures [60], which are still present when non-magnetic dilution is introduced [61], and $Ho_2Zr_2O_7$ displaying features of spin freezing and slow spin-glass dynamics through an analysis of the thermomagnetic data [62,63]. All these previous results boost and address research to start looking for fractionalized quasiparticles, which provide important information about the topological magnetism involved. Instead of magnons, one looks for spinons, monopoles, etc.

Here we present the results of a structural study and thermomagnetic measurements of the terbium zirconate $Tb_2Zr_2O_7$. Even though there is an extensive disorder in the lattice of $Tb_2Zr_2O_7$, it still provides valuable insights when compared with the cooperative spin liquid $Tb_2Ti_2O_7$ or to the glassy $Tb_2Hf_2O_7$. We observe many physical similarities between these two, terbium-based, cubic compounds. Dominant antiferromagnetic interactions are observed with persistent spin dynamics down to mK temperatures. The convergence of the recovered entropy to *R*ln(4) is observed around 30 K. Our results suggest that a spin-glass-like transition occurs at 2.5 K, but the system remains considerably dynamic down to 100 mK. In the presence of an applied magnetic field, the fluctuations are suppressed and a more correlated collective form of magnetism persists.

2. Experimental

Polycrystalline $Tb_2Zr_2O_7$ sample was prepared via the soft-chemistry sol–gel method, providing a simpler route to synthesize pyrochlore oxides at lower temperatures in shorter times than standard powder reactions. It also has the advantage of producing high purity and better homogenization of the powder, at a molecular level [64,65]. Terbium oxide Tb_4O_7 (99.99 %), and alkoxide tetrabutyl zirconate, $C_{16}H_{36}O_4Zr$, were used as precursors of dissolutions containing the cations Tb^{3+} and Zr^{4+}. The mixture of the dissolutions was maintained in stirring until it

became a gel, then this gel was heat-treated at 950 °C for 24 h, see Refs. [62,66] for details. This method was also employed for preparing the nonmagnetic $Lu_2Zr_2O_7$ used in the analysis of the thermal data. X-ray powder-diffraction data was collected with a Shimadzu XRD-7000diffractometer in Bragg-Brentano geometry, using Cu Kα1 radiation (1.5406 Å). Rietveld refinement of the structure from the powder X-ray-diffraction spectrum was performed using the FULLPROF program [67] and the graphical interface WINPLOTR [68].

Magnetic and specific-heat experiments were conducted using a vibrating sample magnetometer and a dilution refrigerator; respectively, both operation modes equipped on a calorimeter Physical Property Measurement System (Quantum Design). The specific heat of the sample holder and Apiezon N grease (addenda) was determined prior to the measurements. ac Magnetic susceptibility measurements were carried out using a PPMS in ac susceptometer option for several frequencies down to 2 K and a home-made ac susceptometer insert in a helium-4 cryostat; operating with a mutual inductance bridge, at a frequency of 155 Hz, all experiments run with an excitation field of 1 Oe.

3. Results and discussion

The X-ray powder-diffraction data found the $Tb_2Zr_2O_7$ sample to be single phase with no additional impurities detected. The structure analysis confirmed that the diffractogram is well described by the cubic defect fluorite with $Fm\bar{3}m$ symmetry as reported previously [69], see Fig. 1. The value of the lattice constant is $a = 5.233(2)$ Å in the refined profile (Table 1), with a goodness-of-fit $\chi^2 = 4.6$. The refinement of a model with the pyrochlore structure and space group $Fd\bar{3}m$ to the data resulted in a poor fit. In the fluorite model, the values of the refined occupancies of the shared 4a site for the Tb and Zr cations resulted in a ~ 50 % of occupancy for each atom, minimizing the possibility of vacancies on these sites. For the 8c site of the O anion, the refined occupancy does not differ from the expected value of 7/8. The reliability of the fitted profile and χ^2 is preserved within an experimental error of the Tb/Zr occupancies smaller than 5 %. In the defect-fluorite lattice, 7 oxygen atoms in the same crystallographic site surround locally the rare-earth cations, distinct from the pyrochlore lattice in which the rare-earth environment is formed by 8 oxygen anions lying on two different crystallographic sites [2,37]. This change in the local structure around the rare-earth atom would suggest a different CEF level scheme of the defect fluorites and of their pyrochlore-related ones. The single-ion magnetic properties and local magnetism are therefore expected to change between $Tb_2Zr_2O_7$ and $Tb_2Ti_2O_7$ (which has two low-lying non-Kramers doublets [23,70]) resulting in changes in the bulk magnetic properties, especially at low temperatures. We could gain some important insights about the CEF of $Tb_2Zr_2O_7$ if we look at a compound with similar local environments around the Tb^{3+} cation. Inelastic neutron scattering (INS) experiments in the isostructural with a complete or high substitution of the cation of Tb by a nonmagnetic cation such Lu must be addressed in future works in order to probe the crystal field states associated within the $Fm\bar{3}m$ fluorite environment. For example, the non-Kramer $Tb_2Hf_2O_7$, which is found at the phase boundary between pyrochlore/defect-fluorite structures [35,36]. In this mixed structure, the unit cell has been reported as a perfect arrangement of the Tb cations in a pyrochlore lattice together with a considerable number of oxygen-Frenkel defects [35], which are described by an empty site (48*f*) and an interstitial oxygen (8*a*). Due to the presence of the Frenkel defect, the local environment of Tb has an oxygen coordination of 7 [35] equal to the average oxygen coordination in the defect fluorite. This occurs for around 50 % of the Tb cations randomly in the $Tb_2Hf_2O_7$ lattice [35]. In the fluorite, the tetrahedra sublattice, albeit with Tb/Zr intermixing, the oxygen coordination around Tb, and the random disorder provide a wide variety of low-temperature properties, as we highlight below (see Table 2).

The inverse of the measured magnetic susceptibility of $Tb_2Zr_2O_7$ and the fit to the Curie-Weiss law are shown in Fig. 2. The linear fit between 10 and 100 K yields a negative Curie-Weiss temperature, $\Theta_{CW} = -9.1(2)$ K, indicating dominant antiferromagnetic interactions. The effective magnetic moment $\mu_{eff} = 9.0(1)\ \mu_B$ is close to the expected value of 9.6 μ_B for free Tb^{3+} ion. The upper inset of Fig. 2 shows the data when fitted in the range of 50 to 300 K which yields a larger value $\Theta_{CW} = -15.1(1)$ K, in good agreement with the antiferromagnetic $\Theta_{CW} = -19$ K and −14.6 K reported for pyrochlores $Tb_2Ti_2O_7$ [17] and $Tb_2Hf_2O_7$ [36]; respectively, in similar high temperature intervals. Deviation from the Curie-Weiss law occurs below 50 K, indicating that spin–spin correlations are significant below this temperature. For $Tb_2Ti_2O_7$, short-range magnetic correlations at temperatures up to 50 K were seen in neutron scattering studies [18]. We must stress the fact that these Curie-Weiss temperatures are only a mean field estimation of a much more complex and realistic scenario involving different exchange constants. The lower inset of Fig. 2 shows magnetization as a function of the applied field at a temperature T = 2 K. The magnetic moment for $Tb_2Zr_2O_7$ reaches 4.5 μ_B/Tb ion at 7 T as reported in previous measurements [17,71] and is in close agreement with the attained values around 5 μ_B/Tb observed in pyrochlores $Tb_2Ti_2O_7$ [72] and $Tb_2Hf_2O_7$ [36].

The temperature dependence of the real part of the ac magnetic susceptibility $\acute{\chi}_{ac}(T)$ for $Tb_2Zr_2O_7$ in zero field is shown in Fig. 3(a). The χ_{ac} values reveal a broad frequency-dependent peak at $\acute{T} \approx 2.5$ K for frequencies between 15 Hz and 10 kHz. It occurs at almost one order of magnitude higher than the glassy-like transitions at 0.75 K and 0.25 K reported for $Tb_2Hf_2O_7$ [35,36] and $Tb_2Ti_2O_7$ [21,73], respectively. The χ_{ac} signal decreases monotonically but does not reach zero at 0.7 K suggesting a slowing down of the spin dynamics, but not complete freezing in $Tb_2Zr_2O_7$. Fig. 3(b) shows the peak in the imaginary part $\acute{\chi}_{ac}$ of the susceptibility, coinciding with $\acute{\chi}_{ac}$ on their temperature positions. Both parts of susceptibility present a non-negligible shift to higher temperatures with increasing frequency, which is a recognizable feature of a spin-glass transition [74].

In the series of the rare-earth zirconates, the disordered fluorites have been constantly reported as having different levels of glassy character [59,60,75]. This is mainly inferred modelling to the ac

Table 1
Refined crystallographic parameters for $Tb_2Zr_2O_7$.

Crystal system	Cubic
Space Group	$Fm\bar{3}m$
a (Å)	5.233(2)
Tb	4a (0,0,0)
Occupancy	0.499(4)
Zr	4a (0,0,0)
Occupancy	0.499(5)
O	8c (0.25,0.25,0.25)
Occupancy	0.92(2)
Number of variables	21
R_{wp} (%)	14.3
R_{exp} (%)	6.6
χ^2	4.6

Table 2
Values of the measured and estimated magnetic parameters.

	$Tb_2Zr_2O_7$
μ_{eff} (μ_B)	9.0(1)
Θ_{CW} (K)	−9.1(2)
χ_{ac} peak at $\acute{T}$ (K)	2.5
Dynamic scaling law	
T_{SG} (K)	2.2
zυ	5.8
τ_0 (s)	2×10^{-8}
Vogel-Fulcher law	
T_0 (K)	1.6
E (K)	15.8
τ_0 (s)	$1x10^{-10}$

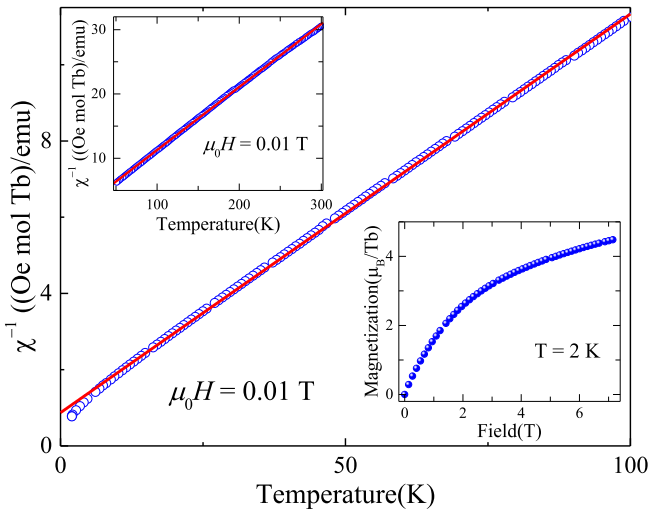

Fig. 2. Inverse susceptibility (χ^{-1}) versus temperature and Curie-Weiss fit to the lowest temperature. Upper inset: χ^{-1} data and the Curie-Weiss fit between 50 and 300 K. Lower inset: magnetization versus the applied magnetic field shows a magnetic moment reaching 4.5 μ_B/ Tb ion at 2 K and 7 T.

susceptibility curves measured at different frequencies. Here we perform an analysis of the peak position centered at $\acute{T}$ for different frequencies f. We obtained the value of the peak temperature shift per decade of frequency $\delta\acute{T} = \Delta\acute{T}/(\acute{T}\,\Delta\log f)$ equal to $\delta\acute{T} = 0.064$. This estimate is close to the values of 0.06 reported for the pyrochlores $Tb_2Ti_2O_7$ and $Tb_2Hf_2O_7$ [29,36], and is considerably higher than that usually found for canonical spin glasses (between 0.005 and 0.01) [74]. The Arrhenius law, $f = f_0\exp(-E_b/\acute{T})$, is used to describe a thermally activated process with a single energy barrier E_b and a characteristic frequency f_0. According to Mydosh [74], this model does not describe canonical spin glasses well; our fit (not shown) to the data returned an energy barrier of $E_b = 98$ K and an unphysical frequency, $f_0 = 10^{19}$ Hz, supporting the spin-glass descriptor of $Tb_2Zr_2O_7$. A common model used to describe spin glasses is the dynamic scaling law expression, $\tau = \tau_0\,((\acute{T}\text{-}\,T_{SG})/T_{SG})^{-z\upsilon}$, where $\tau = 1/2\pi f$ is the characteristic relaxation time, T_{SG} is the peak position as f tends to zero and zυ is the critical exponent. T_{SG} was approximated as 2.2 K, and the fit yields the values of $\tau_0 = 2 \times 10^{-8}$ s and zυ = 5.8. This model describes the data well, as seen in Fig. 4(a), and zυ is in agreement with reported values for spin glasses (zυ = 4–12) [74,76–79]. The second model employed is the phenomenological Vogel-Fulcher law $\tau = \tau_0\exp(-E/(\acute{T}\text{-}T_0))$, where E is the activation energy and T_0 accounts for the interaction between magnetic clusters [74]. We obtained the parameters, $\tau_0 = 1\text{x}10^{-10}$ s, $E = 15.8$ K and $T_0 = 1.6$ K. Fig. 4(b) depicts the best fit to the Vogel-Fulcher law, the obtained T_0 is smaller than $\acute{T} \approx 2.5$ K,

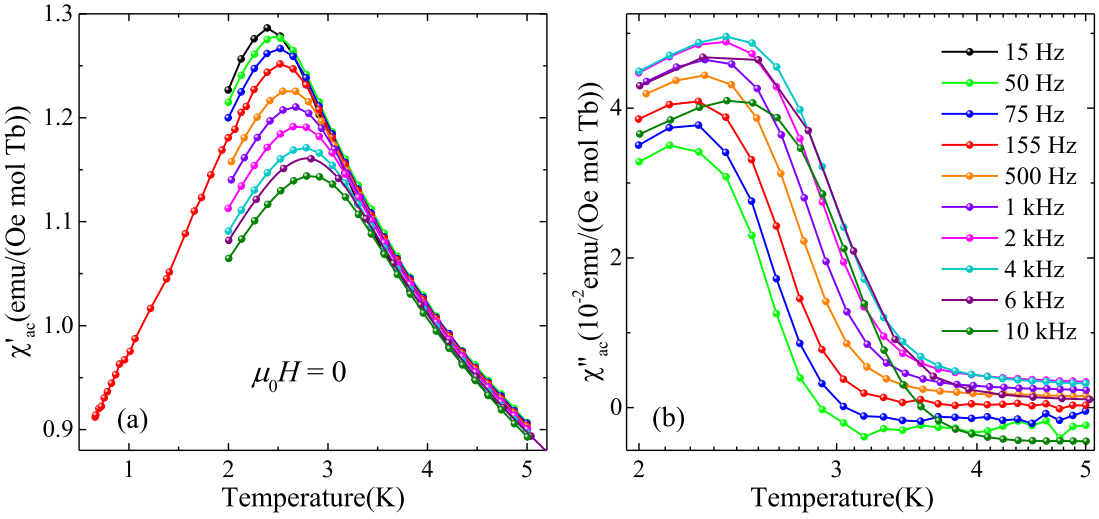

Fig. 3. Temperature dependence of the real part of the ac magnetic susceptibility $\acute{\chi}_{ac}$ in zero magnetic field for $Tb_2Zr_2O_7$. There is a magnetic anomaly around the temperature $\acute{T} \approx 2.5$ K. Temperature dependence of the imaginary part of the ac magnetic susceptibility $\acute{\chi}_{ac}$ in zero field.

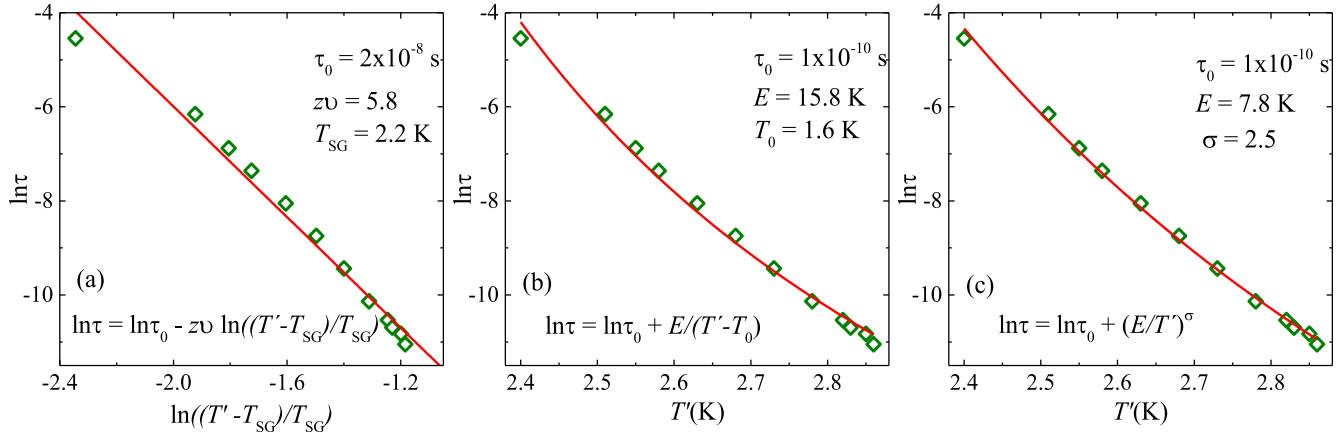

Fig. 4. Logarithmic spin-relaxation time lnτ fitted to the dynamical scaling law (a), to the Vogel-Fulcher law (b), and to the equation $\tau = \tau_0\exp[(E/\acute{T})^{\sigma}]$ (c).

although they are expected to be similar, $T_0 \approx \acute{T}$, for canonical spin glasses [74]. In spite of that, our results show pieces of evidence for the presence of an unusual spin freezing in $Tb_2Zr_2O_7$. Following the same study for the glassy behavior reported in $Tb_2Ti_2O_7$ [29], the f dependence of $\acute{T}$ was modeled by a power law of the Arrhenius relation $\tau = \tau_0 \exp[(-E/\acute{T})^{\sigma}]$. The fit provides an excellent description of the data, as displayed in Fig. 4(c). The fit results in values of $\tau_0 = 1 \times 10^{-10}$ s, $E = 7.8$ K and $\sigma = 2.5$. For $Tb_2Ti_2O_7$, such a fit yields $\tau_0 = 1.1 \times 10^{-9}$ s, $E = 0.91$ K and $\sigma = 2$ [29].

The ac susceptibility data reveal evidence for a slowing down of the spin dynamics below 2.5 K, and the obtained parameters suggest that the magnetic correlations have a glassy nature. In $Tb_2Zr_2O_7$, the large number of non-magnetic defects or disorder in the lattice leads to a spin-glass-like transition similar to what is observed for $Tb_2Hf_2O_7$ possessing oxygen-disordered defects [35], but at a higher energy scale. This is an interesting result for experimental research, and since the presence of glassy features together with an intrinsic disorder related to the random Tb/Zr occupation of the lattice can host localized fractional excitations [80].

In the presence of a dc applied magnetic field, we measured the real part of the ac susceptibility at 1 kHz and 10 kHz and the results are shown in Fig. 5. The application of a field causes a drop in the susceptibility peak in almost an order of magnitude. More interestingly, an additional bump of the same height of the former begins to emerge at 3.5 T. At a field strength higher than 5 T, we observe a clear emergence of a second peak at ~ 25 K, which shifts to higher temperatures with increasing field. The behavior persists up to 9 T and a frequency of 10 kHz. This peak is reminiscent of the one found in the in-field $\chi_{ac}(T)$ at ~ 20 K reported for $Tb_2Ti_2O_7$ which was associated with field-induced polarized spins in its paramagnetic state [30]. The measured in-field peak is due to the magnetic moments of Tb^{3+}, which possess a value close to 5 μ_B from our magnetization measurements (inset Fig. 2). A contribution to susceptibility associated with spin fluctuations in a strong enough field is ruled out, since it must approximates to zero at high temperatures and close to 0 K. Our data at the 25 K peak appears to exhibit no frequency dependence in the kHz range. However, more experiments are required to verify the existence of frequency dependence of this in-field peak and the possible time scales of the associated spin relaxation. The characterization of the relaxation of the spins at higher temperatures could open a discussion of a possible spin-glass state. Despite the disorder in the lattice, there is a presumable similar magnetic dipolar coupling as in the pyrochlore $Tb_2Ti_2O_7$ reported with an unusual slow spin relaxation [30]. Correlated domains of spins and slow dynamics similar to ferromagnetic cluster systems have been discussed for $Tb_2Ti_2O_7$ [30]. The disorder in the lattice of $Tb_2Zr_2O_7$ and our measurements reveal evidence of a slowing down of spin fluctuations, similar to that seen in non-magnetic dilution studies of the Tb sublattice in $Tb_2Ti_2O_7$ reported in [81]. The in-field data of the imaginary part of the ac susceptibility (not shown) is too noisy to be discussed.

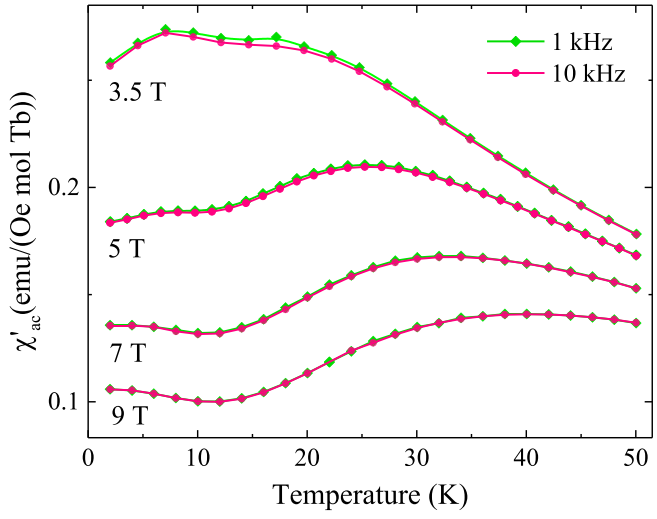

Fig. 5. The temperature dependence of $\acute{\chi}_{ac}$ for $Tb_2Zr_2O_7$ in various applied fields at different frequencies. There is an emergence of a peak at ≈ 25 K for field values higher than 3.5 T.

Measurements of the total specific heat C as a function of the temperature were carried out in different applied magnetic fields, as shown in Fig. 6. The data does not display sharp features down to 100 mK that would arise from a long-range ordering, but exhibit a broad peak centered at about 5 K. The maximum at 5 K has a reduced amplitude and shares some resemblance if compared to $Tb_2Ti_2O_7$ as reported in [17]; also, a similar broad feature is exhibited in lower temperatures and around 2 K for $Tb_2Hf_2O_7$ [35], and attributed to short-range spin correlations in both systems. Thereby, the upturn below 20 K suggests the inception of magnetic correlations that does not reach long-range ordering. Additional maxima reported at temperatures below 2 K for the highly sample-dependent pyrochlore $Tb_2Ti_2O_7$ [17,73,82,83] are absent in our disordered fluorite. The absence of a feature in specific heat around the spin freezing temperature of 2.5 K is a characteristic signature of canonical spin glasses [43,84]. The application of increasing magnetic fields causes the single peak shifts to higher temperatures and around a 3.5 T field the peak becomes much broader in temperature. The upturn of C below 0.5 K is attributed to the nuclear specific heat C_N, which was accounted for by calculating the nuclear specific heat of terbium metal (C_{TbMet}) for the isotope ^{159}Tb with the nuclear spin $I = 3/2$, hyperfine constant $A = 0.15$ K and quadrupole coupling constant $P = 0.021$ K [85]. For avoiding inconsistent results in the low-temperature region of the data, we used the reduced nuclear-specific heat $C_N = f^*$ x C_{TbMet} ($f^* = 0.6$). The parameter f^* is a reduction factor which is less than one, and represents the fraction of Tb spins with full magnetic moment ($\mu_{Tb} = 10\ \mu_B$). This method has been employed for estimating successfully the nuclear contribution in thermal analyses for praseodymium pyrochlores [57,86]. Another estimate to the nuclear term (not shown) was approached considering reduced magnetic moments of $0.55\mu_{Tb}$, but the data is not reproduced as fairly as with the C_N curve. However, more measurements below 100 mK are required to confirm the moment of Tb in the disordered fluorite. The reduction factor introduced is due to the electronic magnetic moments smaller than the

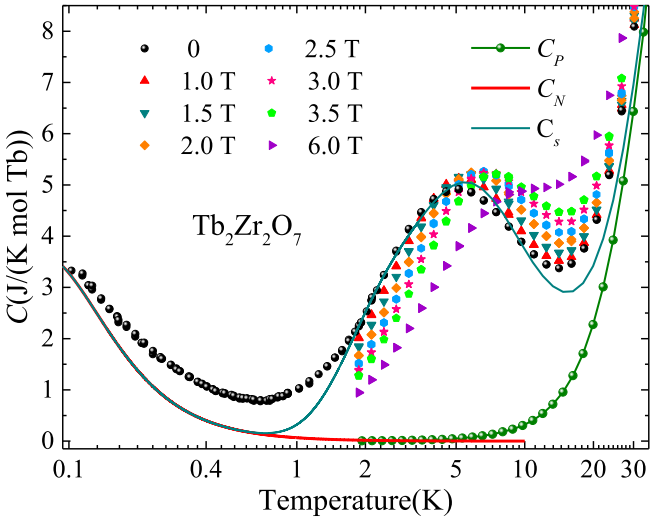

Fig. 6. Total specific heat C as a function of temperature for $Tb_2Zr_2O_7$ in different applied magnetic fields. The specific heat of the isostructural nonmagnetic $Lu_2Zr_2O_7$ (C_P) and the computed nuclear specific heat (C_N) are marked by green and redlines, respectively. C_s represents the sum of the lattice, nuclear and CEF contributions to the specific heat measured at zero field. (For interpretation of the references to colour in this figure legend, the reader is referred to the web version of this article.)

saturated value which are acting on the nuclear moments, reflecting spin fluctuations [87,88]. This supports a model of reduced moments and it is associated with quantum spin fluctuations affecting the nuclear spins [87,88]. This was also revealed by the large values of susceptibility χ_{ac} at the lowest temperature measured. Our results, suggesting a frozen moment along with fluctuations are rich ingredients for the theory proposed for topological spin glasses by Sen and Moessner [80]. The lattice specific heat C_p of our system is prominent at temperatures above 10 K and does not exhibit a strong field dependence, it was approximated by measuring the specific heat of the nonmagnetic fluorite $Lu_2Zr_2O_7$.

The lattice and nuclear contributions to the specific heat of $Tb_2Zr_2O_7$ were subtracted from its total specific heat to isolate the electronic magnetic specific-heat C_e. In Fig. 7, by integrating numerically the $C_e(T)/T$ data at zero field, we obtained the change of the electronic magnetic entropy ΔS_e. Above 18 K, the values of ΔS_e are higher than the entropy due to a two-level ground state: Rln(2), and reveal that this is a high enough temperature to recover an entropy associated with two lowest doublets: Rln(4). This result is similar to the value of the recovered entropy reported for $Tb_2Ti_2O_7$ [17,73]. This scenario probably suggests a ground state of two doublets but measurements of the CEF levels are required to clarify this assumption. Close to 75 % of the limit entropy is released above the freezing temperature of 2.5 K which is a unique characteristic of a spin-glass phase transition [43]. The fact that the entropy is slightly below Rln(4) could be an indication that short-range correlations are still present at high temperatures.

In Fig. 8 we plot the in-field specific heat divided by the temperature $C_e(T)/T$. The broad maxima below 5 K can be associated with the population of CEF levels similarly to the one found in $Tb_2Ti_2O_7$ [17]. Furthermore, in the disordered structure of $Tb_2Hf_2O_7$, the specific heat near 50 K displays a Schottky anomaly [36]. The scheme of a three-level CEF was determined to be in close agreement within the energy scale of a broad CEF spectra reported from INS [36]. In this framework, we try for our data the expression for the CEF-specific heat considering a three-level system [89]. The fitted curves (solid lines) indicate the CEF contribution (C_{CEF}), which described fairly well the data for a doublet ground state, with a first excited doublet below 10 K (energy gap $\Delta\varepsilon_1$), and a quartet state at around 20 K ($\Delta\varepsilon_2$). For example, at zero field, the obtained $\Delta\varepsilon_1$ is equal to 7.4 K, which is much smaller compared to the gap value of 17 K between the two non-Kramers doublets in $Tb_2Ti_2O_7$ [17,18,70], suggesting a closer distribution of energy levels. This result may be associated to the randomness effect around Tb^{3+}, similarly to the observed fact that defects in $Tb_2Hf_2O_7$ lead to a broad CEF excitation

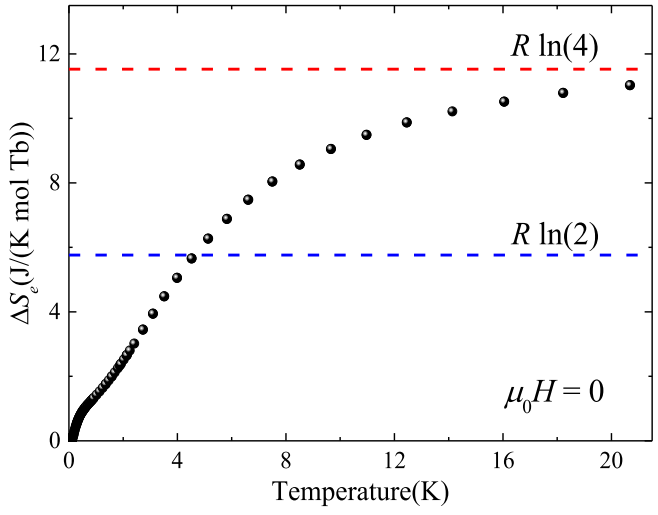

Fig. 7. Electronic magnetic entropy $\Delta S_e(T)$ at zero field. The dashed lines denote the entropy for a system with a two-level (Rln(2)) and a two-doublets (Rln(4)) scheme.

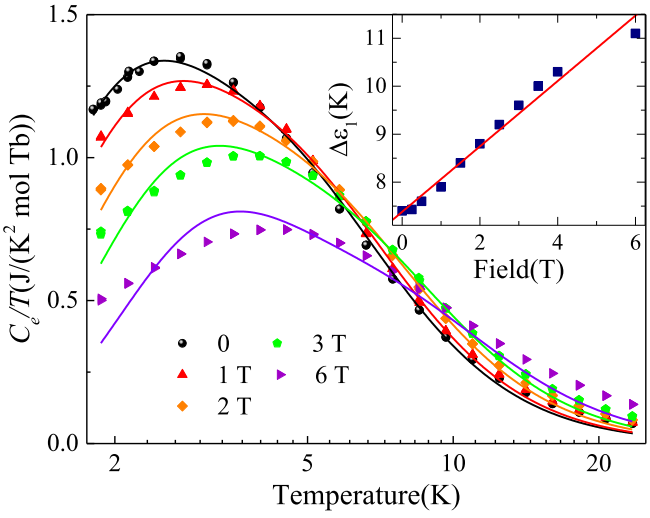

Fig. 8. Electronic magnetic specific heat divided by the temperature $C_e/T(T)$ in magnetic fields up to 6 T. Solid lines are the three-level fits. Inset: Energy gap values between the first excited level and ground state ($\Delta\varepsilon_1$) as a function of the applied field.

signal built from groups of crystal-field environments surrounding the cation [35]. The value of the first crystal electric field splitting is close to the energy scale of the broad maxima, and then its origin is the thermal population of CEF levels. For the in-field data, the three-level fit continues to reproduce well the width and the position of the peak. The inset of Fig. 8 shows the linear dependence of $\Delta\varepsilon_1$ with the applied magnetic field (H). The data were fitted using the expression for the Zeeman separation such $\Delta\varepsilon_1 = (g\mu_B/k_B)H$ for an effective spin $S = 1/2$, where the average g-factor is a fitting parameter. The value of the obtained factor $g = 1.0(1)$ is almost a tenth of the factor parallel to the trigonal Ising axis $g_{//} = 9.6$ ($g = 0$) found in $Tb_2Ti_2O_7$ [70]. However, the estimated g-factor of $Tb_2Zr_2O_7$ is close to the factors along the local trigonal axis reported for XY pyrochlores: $Er_2Ti_2O_7$ ($g_{//} = 1.8$, $g = 7.7$) and $Yb_2Ti_2O_7$ ($g_{//} = 2.0$, $g = 4.1$) [70], known for having a strong planar CEF anisotropy. Diffuse magnetic scattering and modeling results on the defect $Tb_2Hf_2O_7$ rule out Tb^{3+} spins with Ising anisotropy but a quality fit was obtained by considering isotropic spins with antiferromagnetic correlations as reported by Sibille *et al.* and Anand *et al* [36]. These results indicate that a potential first model for the low-temperature magnetic state in $Tb_2Zr_2O_7$ could be spins randomly oriented with short antiferromagnetic correlations consistent with models found in $Tb_2Ti_2O_7$ [19] and in $Dy_2Zr_2O_7$ [60]. If these correlations extend over many tetrahedra, we could possibly be entering a spin configuration in which phase competitions are present as observed in XY pyrochlores [90]. Hallas *et al.* [90] discussed this picture of the ground state for XY pyrochlores supported by the presence of a broad specific heat anomaly together with no magnetic ordering at lower temperatures, which are physical signatures found in the defect-fluorite $Tb_2Zr_2O_7$. The scenario pictured here for $Tb_2Zr_2O_7$ must be confirmed by neutron experiments to determine the size and anisotropy of the Tb^{3+} magnetic moment in its ground state, and by Mössbauer spectroscopy to evidence spin fluctuations at the very low temperatures as suggest by our specific heat measurements.

4. Conclusion

Polycrystalline samples of $Tb_2Zr_2O_7$ were sintered successfully using the sol–gel method. From its time correlations and parameters obtained from spin-glass models, we identified a spin-glass-like transition at ~ 2.2 K in $Tb_2Zr_2O_7$. Specific heat revealed no long-range order and the presence of spin fluctuations in the mK scale, with the moments fluctuating rapidly due to strong magnetic frustration. We found several

similarities in the properties of $Tb_2Zr_2O_7$ and other terbium pyrochlore oxides, $Tb_2Ti_2O_7$ and $Tb_2Hf_2O_7$, with the later been shown to display a glassy-like transition [36]. Our data suggest a new form of collective behavior in the presence of strong magnetic fields which induces a possible spin relaxation (because of the high dynamics), contrary to the standard intuition that a strong field would accelerate relaxation to an equilibrium state. To provide more information about the cooperative state or the glassy-like correlations of $Tb_2Zr_2O_7$, different probes like μSR are required to observed the moment fluctuations rates of Tb^{3+} and their respective slowing down below the temperature of the susceptibility peak.

Declaration of Competing Interest

The authors declare that they have no known competing financial interests or personal relationships that could have appeared to influence the work reported in this paper.

Data availability

Data will be made available on request.

Acknowledgments

R. S. Freitas acknowledges FAPESP (Grant No.2015/161915) and CNPq (Grant No. 429511/2018-3).

References

[1] C. Lacroix, P. Mendels, F. Mila, Introduction to Frustrated Magnetism: Materials, Experiments, Theory, Springer-Verlag, Berlin, 2011.
[2] J.S. Gardner, M.J.P. Gingras, J.E. Greedan, Rev. Mod. Phys. 82 (2010) 53.
[3] H.T. Diep, Frustrated Spin Systems, World Scientific, Singapore, 2013.
[4] L. Balents, Nature 464 (2010) 199.
[5] L. Savary, L. Balents, Rep. Progress Phys. 80 (2017), 016502.
[6] A. Kluber, T.A. Burt, C. Clementi, Proc. Natl. Acad. Sci. U.S.A. 115 (2018) 9234.
[7] A.P. Ramirez, A. Hayashi, R.J. Cava, R. Siddharthan, B.S. Shastry, Nature (London) 399 (1999) 333.
[8] B.C. den Hertog, M.J.P. Gingras, Phys. Rev. Lett. 84 (3430) (2000) pp.
[9] C. Castelnovo, R. Moessner, S.L. Sondhi, Nature 451 (2008) 42.
[10] L.D.C. Jaubert, P.C.W. Holdsworth, J. Phys.: Condens. Matter 23 (2011), 164222.
[11] L. Savary, K.A. Ross, B.D. Gaulin, J.P.C. Ruff, L. Balents, Phys. Rev. Lett. 109 (167201) (2012) pp.
[12] M.E. Zhitomirsky, M. Gvozdikova, P.C.W. Holdsworth, R. Moessner, Phys. Rev. Lett. 109 (077204) (2012) pp.
[13] J.D.M. Champion, A.S. Wills, T. Fennell, S. Bramwell, J. Gardner, M. Green, Phys. Rev. B 64 (140407) (2001) pp.
[14] J.R. Stewart, G. Ehlers, A. Wills, S.T. Bramwell, J.S. Gardner, J. Phys.: Condens. Matter 16 (L321) (2004) pp.
[15] K. Ross, L. Savary, B. Gaulin, L. Balents, Phys. Rev. X 1 (021002) (2011) pp.
[16] A. Scheie, J. Kindervater, S. Zhang, H.J. Changlani, G. Sala, G. Ehlers, A. Heinemann, G.S. Tucker, S.M. Koohpayeh, C. Broholm, Proc. Natl. Acad. Sci Usa 117 (2020) 27245.
[17] M.J.P. Gingras, B.C. den Hertog, M. Faucher, J.S. Gardner, S.R. Dunsinger, L. J. Change, B.D. Gaulin, N.P. Raju, J.E. Greedan, Phys. Rev. B 62 (2000) 6496.
[18] J.S. Gardner, S.R. Dunsinger, B.D. Gaulin, M.J.P. Gingras, J.E. Greedan, R.F. Kiefl, M.D. Lumsden, W.A. MacFarlane, N.P. Raju, J.E. Sonier, I. Swainson, T. Z., Phys. Rev. Lett., vol. 82, p. 1012, 1999.
[19] J.S. Gardner, B.D. Gaulin, A.J. Berlinsky, P. Waldron, S.R. Dunsiger, N.P. Raju, J. E. Greedan, Phys. Rev. B 64 (2001), 224416.
[20] T. Fennell, M. Kenzelmann, B. Roessli, M.K. Haas, R.J. Cava, Phys. Rev. Lett. 109 (017201) (2012) pp.
[21] J.S. Gardner, A. Keren, G. Ehlers, C. Stock, E. Segal, J.M. Roper, B. Fak, M.B. Stone, P.R. Hammar, D.H. Reich, B.D. Gaulin, Phys. Rev. B 68 (2003) 180401(R).
[22] J. Zhang, K. Fritsch, Z. Hao, B.V. Bagheri, M.J.P. Gingras, G.E. Granroth, P. Jiramongkolchai, R.J. Cava, B.D. Gaulin, Phys. Rev. B 89 (2014), 134410.
[23] A.J. Princep, H.C. Walker, D.T. Adroja, D. Prabhakaran, A.T. Boothroyd, Phys. Rev. B 91 (2015), 224430.
[24] T. Fennell, O.A. Petrenko, B. Fak, S.T. Bramwell, M. Enjalran, T. Yavors'kii, M.J.P. Gingras, R.G. Melko, G. Balakrishnan, Phys. Rev. B, vol. 70, p. 134408, 2004.
[25] M.J. Harris, S.T. Bramwell, D.F. McMorrow, T. Zeiske, K.W. Godfrey, Phys. Rev. Lett. 79 (1997) 2554.
[26] S.T. Bramwell, M.J. Harris, B.C. Den Hertog, M.J.P. Gingras, J.S. Gardner, D. F. McMorrow, A.R. Wildes, A.L. Cornelius, J.D.M. Champion, R.G. Melko, T. Fennell, Phys. Rev. Lett. 87 (2001), 047205.
[27] H.R. Molavian, M.J.P. Gingras, B. Canals, Phys. Rev. Lett. 98 (2007), 157204.
[28] G. Luo, S.T. Hess, C.L.R., Phys. Lett. A, vol. 291, p. 306, 2001.
[29] E. Lhotel, C. Paulsen, P. Dalmas de Ŕeotier, A. Yaouanc, C. Marin, S. Vanishri, Phys. Rev. B, vol. 86, no. 020410(R), 2012.
[30] B.G. Ueland, G.C. Lau, R.J. Cava, J.R. ÓBrien, P. Schiffer, Phys. Rev. Lett., vol. 96, no. 027216, 2006.
[31] T. Taniguchi, H. Kadowaki, H. Takatsu, B. Fåk, J. Ollivier, T. Yamazaki, T. Sato, H. Yoshizawa, Y. Shimura, T. Sakakibara, T. Hong, K. Goto, L. Yaraskavitch, J. Kycia, Phys. Rev. B vol. 87, no. 060408(R) (2013).
[32] H. Kadowaki, M. Wakita, B. Fåk, J. Ollivier, S. Ohira-Kawamura, K. Nakajima, J. W. Lynn, Phys. Rev. B 99 (014406) (2019) pp.
[33] J. Rau, M. Gingras, Annu. Rev. Condens. Matter Phys. 10 (2019) 357.
[34] G. Sala, M.J. Gutmann, D. Prabhakaran, D. Pomaranski, C. Mitchelitis, J.B. Kycia, D.G. Porter, C. Castelnovo, J.P. Goff, Nat. Mater 13 (488) (2014) pp.
[35] R. Sibille, E. Lhotel, M.C. Hatnean, G.J. Nilsen, G. Ehlers, A. Cervellino, E. Ressouche, M. Frontzek, O. Zaharko, V. Pomjakushin, U. Stuhr, H.C. Walker, D. T. Adroja, H. Luetkens, C. Baine, A. Amato, G. Balakrishnan, T. Fennell, M. Kenzelmann, Nat. Commun. 8 (892) (2017) pp.
[36] V.K. Anand, L. Opherden, J. Xu, D.T. Adroja, A.D. Hillier, P.K. Biswas, T. Herrmannsdörfer, M. Uhlarz, J. Hornung, J. Wosnitza, E. Canévet, B. Lake, Phys. Rev. B 97 (094402) (2018) pp.
[37] M.A. Subramanian, G. Aravamudan, G.V. Subba Rao, Prog. Solid State Chem. 15 (1983) 55.
[38] G.C. Lau, B.D. Muegge, T.M. McQueen, E.L. Duncan, R.J. Cava, J. Solid State Chem. 179 (2006) 3126.
[39] G.C. Lau, R.S. Freitas, B.G. Ueland, B.D. Muegge, E.L. Duncan, P. Schiffer, R. J. Cava, Nat. Phys. 2 (2006) 249.
[40] B. Paul, K. Singh, T. Jaron, A. Roy, A. Chowdhury, J. Alloys Compd. 686 (2016) 130.
[41] J.M. Longo, P.M. Raccah, J.B. Goodenough, Mater. Res. Bull. 4 (1969) 191.
[42] A. Menushenkov, V. Popov, B.R. Gaynanov, I.A.A., A. Kuznetsov, A. Yaroslavtsev, F. d'Acapito and A. Puri, JETP Lett., Vols. 109,8, p. 529, 2019.
[43] J.A. Mydosh, Rep. Prog. Phys., vol. 78, no. 052501, 2015.
[44] S.R. Dunsiger, R.F. Kiefl, K.H. Chow, B.D. Gaulin, M.J.P. Gingras, J.E. Greedan, A. Keren, K. Kojima, G.M. Luke, W.A. MacFarlane, N.P. Raju, J.E. Sonier, Y. J. Uemura, W.D. Wu, Phys. Rev. B 54 (13) (1996) 9019.
[45] M.J.P. Gingras, C. Stager, N.P. Raju, B.D. Gaulin, J.E. Greedan, Phys. Rev. Lett. 78 (5) (1997) 947.
[46] J.S. Gardner, B.D. Gaulin, S.-H. Lee, C. Broholm, N.P. Raju, J.E. Greedan, Phys. Rev. Lett. 83 (211) (1999) pp.
[47] J.S. Gardner, G. Ehlers, R.H. Heffner, F. Mezei, J. Magn. Magn. Mater 226–230 (2001) 460.
[48] H.J. Silverstein, K. Fritsch, F. Flicker, A.M. Hallas, J.S. Gardner, Y. Qiu, G. Ehlers, A.T. Savici, Z. Yamani, K.A. Ross, B.D. Gaulin, M.J.P. Gingras, J.A.M. Paddison, K. Foyevtsova, R. Valenti, F. Hawthorne, C.R. Wiebe, H.D. Zhou, Phys. Rev. B 89 (054433) (2014) pp.
[49] K. Miyoshi, K. Honda, T. Yamashita, K. Fujiwara, J. Takeuchi, J. Magn. Magn. Mater 226–230 (2001) 898.
[50] G. Ehlers, J.E. Greedan, J.R. Stewart, K.C. Rule, P. Fouquet, A.L. Cornelius, C. Adriano, P.G. Pagliuso, Y. Qiu, J.S. Gardner, Phys. Rev. B 81 (224405) (2010) pp.
[51] D.K. Singh, Y.S. Lee, Phys. Rev. Lett. 109 (247201) (2012) pp.
[52] E.C. Andrade, J.A. Hoyos, S. Rachel, M. Vojta, Phys. Rev. Lett. 120 (097204) (2018) pp.
[53] A. Sharma, A. Young, Phys. Rev. B 83 (214405) (2011) pp.
[54] A. Sharma, A. Young, Phys. Rev. B 84 (014428) (2011) pp.
[55] E. Lhotel, S. Petit, S. Guitteny, O. Florea, M.C. Hatnean, C. Colin, E. Ressouche, M. Lees, G. Balakrishnan, Phys. Rev. Lett. 115 (197202) (2015) pp.
[56] S. Petit, E. Lhotel, B. Canals, M. Hatnean, J. Ollivier, H. Mutka, E. Ressouche, A. Wildes, M. Lees, G. Balakrishnan, Nat. Phys. 12 (2016) 746.
[57] K. Kimura, S. Nakatsuji, J.-J. Wen, C. Broholm, M. Stone, E. Nishibori, H. Sawa, Nat. Commun. 4 (1934) 2013.
[58] J.-J. Wen, S.M. Koohpayeh, K.A. Ross, B.A. Trump, T.M. McQueen, K. Kimura, S. Nakatsuji, Y. Qiu, D. Pajerowski, J.R.D. Copley, C.L. Broholm, Phys. Rev. Lett. 118 (107206) (2017) pp.
[59] K. Vlášková, R.H. Colman, P. Proschek, J. Capek, M. Klicpera, Phys. Rev. B 100 (2019), 214405.
[60] J.G.A. Ramon, C.W. Wang, L. Ishida, P.L. Bernardo, M.M. Leite, F. Vichi, J. S. Gardner, R.S. Freitas, Phys. Rev. B 99 (214442) (2019) pp.
[61] A. Sheetal, S. Ali, Y. Rajput, T.M. Singh, C.S. Yadav, J. Phys.: Condens. Matter 32 (365804) (2020) pp.
[62] J.G.A. Ramon, Doctoral Thesis, Universidade de São Paulo, São Paulo, 2020.
[63] Sheetal, A. Elghandour, R. Klingeler, C. S. Yadav, arXiv:2110.04555, 2021.
[64] L.L. Hench, J.K. West, Chem. Rev. 90 (1990) 33.
[65] J.D. Mackenzie, J. Non-Cryst. Solids 48 (1982) 1.
[66] A. Garbout, S. Bouattour, A.W. Kolsi, J. Alloys Compd. 469 (2009) 229.
[67] J. Rodríguez-Carvajal, Physica B 192 (1993) 55.
[68] T. Roisnel, J. Rodríguez-Carvajal, Mater. Sci. Forum 378–381 (2001) 118.
[69] E. Reynolds, P.E.R. Blanchard, B.J. Kennedy, C.D. Ling, S. Liu, M. Avdeev, Z. Zhang, G.J. Cuello, A. Tadich, L.Y. Jang, Inorg. Chem. 52 (2013) 8409.
[70] A. Bertin, Y. Chapuis, P. Dalmas de Réotier, A. Yaouanc, J. Phys.: Condens. Matter 24 (2012), 256003.
[71] A. Kuznetsov, O.A. Churkin, V. Popov, I.V. Shchetinin, A. Ivanov, A. Yastrebtsev, B. Gaynanov, A. Yaroslavtsev, O. Chernysheva, F. d'Acapito, A. Puri, P. Alekseev, A. Menushenkov, J. Supercond. Nov. Magn. 33 (2020) 2395.
[72] I. Mirebeau, P. Bonville, M. Hennion, Phys. Rev. B 76 (2007), 184436.
[73] N. Hamaguchi, T. Matsushita, N. Wada, Y. Yasui, M. Sato, Phys. Rev. B 69 (2004), 132413.

[74] J.A. Mydosh, Spin Glasses: An experimental Introduction, Taylor & Francis, London, 1993.
[75] M.E.A. Sheetal, R. Klingeler, C.S. Yadav, J. Phys.: Condens. Matter 34 (2022), 245801.
[76] W. Zhang, Y. Sun, H. Wang, Y. Li, X. Zhang, Y. Sui, H. Luo, F. Meng, Z. Qian and G. W, J. Alloys Compd., vol. 589, p. 230, 2014.
[77] L. Xue, L. Shao, Q. Luo, B. Shen, J. Alloys Compd. 790 (2019) 633.
[78] X. Xiao, X. Zhao, J. Guo, W. Liu, Z. Zhang, J. Alloys Compd. 816 (152678) (2020) pp.
[79] Y. Li, X. Kan, X. Liu, S. Feng, Q. Lv, K.M.U. Rehman, W. Wang, C. Liu, X. Wang, Y. Xu, J. Alloys Compd. 852 (156962) (2021) pp.
[80] A. Sen, R. Moessner, Phys. Rev. Lett. 114 (247207) (2015) pp.
[81] A. Keren, J.S. Gardner, G. Ehlers, A. Fukaya, E. Segal, Y. Uemura, Phys. Rev. Lett. Vols. 92,10, no. 107204 (2004).
[82] A. Yaouanc, P. Dalmas de Réotier, Y. Chapuis, C. Marin, S. Vanishri, D. Aoki, B. Fåk, L. -P. Regnault, C. Buisson, A. Amato, C. Baines, Hillier and A. D., Phys. Rev. B, vol. 84, p. 184403, 2011.
[83] H. Takatsu, H. Kadowaki, T.J. Sato, J.W. Lynn, Y. Tabata, T. Yamazaki, K. Matsuhira, J. Phys.: Condens. Matter 24 (2012), 052201.
[84] G. Brodale, R. Fisher, W. Fogle, N. Philips, J. van Curen, J. Magn. Magn. Mater 31–4 (1983) 1331.
[85] O.V. Lounasmaa, P.R. Roach, Phys. Rev. 128 (2) (1962) 622.
[86] Y. Tokiwa, J.J. Ishikawa, S. Nakatsuji, P. Gegenwart, Nat. Mater. 13 (2014) 356–359.
[87] E. Bertin, P. Bonville, J.-P. Bouchaud, J. Hodges, J. Sanchez, P. Vulliet, Eur. Phys. J. B 27 (2002) 347.
[88] P. Bonville, J. Phys. Conf. Ser. 217 (012119) (2010) pp.
[89] H.L. Che, Z.Y. Zhao, X. Rao, L.G. Chu, N. Li, W.J. Chu, P. Gao, X.Y. Yue, Y. Zhou, Q. J. Li, Q. Huang, E.S. Choi, Y.Y. Han, Z.Z. He, H.D. Zhou, X. Zhao, X.F. Sun, Phys. Rev. Mater. 4 (054406) (2020) pp.
[90] A.M. Hallas, J. Gaudet, B.D. Gaulin, Annu. Rev. Condens. Matter Phys. 9 (2018) 105.